

# A Method of Measuring Cosmic Magnetic Fields with Ultra High Energy Cosmic Ray Data

Martin Erdmann, Peter Schiffer

*Physics Institute 3A, RWTH Aachen University, 52056 Aachen, Germany*

---

## Abstract

We present a method to measure cosmic magnetic fields with ultra high energy cosmic rays (UHECRs). We apply an advanced autocorrelation method to simulated UHECRs which includes their directional as well as energy information. Without explicit knowledge of the UHECR sources, such measurements are sensitive to the number of sources and to the magnetic field strength subjected to the UHECRs. Using a UHECR Monte Carlo model including sources and random walk propagation, we explain the procedure of reconstructing the allowed phase space of the model parameters from a simulated autocorrelation measurement.

*Key words:* Autocorrelation, Cosmic Rays, Magnetic Fields

*PACS:* 98.35.Eg, 98.62.En, 98.70.Sa

---

## 1. Introduction

Recent results of the Pierre Auger Observatory [1, 2] show a correlation of ultra high energy cosmic rays (UHECRs) above 56 EeV with nearby active galactic nuclei (AGN) at distances up to 75 Mpc. The exact origin of the UHECRs and the positions of their sources still remain unknown but it is favored that UHECRs are accelerated at discrete sources.

The UHECRs propagate through extragalactic and galactic magnetic fields, and consequently carry information about the direction and strength of the fields. For UHECRs originating from a single source with energies above a certain threshold, the influence of the fields is expected to result in an energy ordering with respect to the direction of the source.

Galactic magnetic fields are known to some extent, from different measurement methods. For recent reviews refer to, e.g. [3, 4]. Information about extragalactic fields exists for a number of galaxy clusters, however, the knowledge of magnetic fields in filaments is uncertain to at least three orders of magnitude [5, 6, 7]. Measurements of UHECRs therefore have good potential of providing additional information on these magnetic fields.

---

*Email address:* schiffer@physik.rwth-aachen.de (Peter Schiffer)

In this contribution we present a new method of obtaining information on the magnetic fields without prior knowledge of the source positions. This is achieved by a statistical approach based on the concept of energy dependent angular ordering of the UHECRs mentioned above. This publication is organized as follows. First we define an energy-energy-correlation observable used to measure the angular ordering. Then we explain the analysis procedure, and demonstrate its application using a Monte Carlo generated UHECR scenario. Finally, we present a method to test models of UHECR emission and propagation using a simulated energy-energy-correlation measurement. In this context we reconstruct the two parameters of a random walk model which are the number of sources emitting UHECRs, and the overall magnetic field strength.

## 2. Definition of Energy-Energy-Correlations

Energy-energy-correlations are a well known quantity from high energy physics, see e.g. [8]. Their definition usually includes the energies and the angular distances of particles, which enables investigation of energy ordering in the UHECR sky. We define the energy-energy-correlation  $\Omega_{ij}$  between the UHECRs  $i$  and  $j$  by

$$\Omega_{ij} = \frac{(E_i(\alpha_i) - \langle E(\alpha_i) \rangle)(E_j(\alpha_j) - \langle E(\alpha_j) \rangle)}{E_i(\alpha_i)E_j(\alpha_j)}. \quad (1)$$

Here  $E_i$  is the energy of the UHECR  $i$ , and  $\alpha_i$  denotes its angular distance with respect to the center of a region of interest (ROI) (figure 1). The ROI covers a limited solid angle and will be precisely outlined in section 3.2.  $\langle E(\alpha_i) \rangle$  denotes the corresponding average energy value of the UHECRs arriving within the same ring interval relative to the ROI center.

Using  $\Omega_{ij}$ , angular ordering of the UHECRs is measured in the following sense,

1. A pair of UHECRs, one being above and the other below the corresponding average energy values, results in a negative correlation  $\Omega_{ij} < 0$ . This is a typical case for a background contribution.
2. A pair with both UHECRs having energy values above or below the average energy value at their corresponding angular distance gives a positive correlation  $\Omega_{ij} > 0$ . Here signal UHECRs are expected to contribute.

This means we expect overall larger  $\Omega_{ij}$  for a mixing of coherently arriving UHECRs from a source with background UHECRs, than for an exclusively isotropic arrival. In this way, the energy-energy-correlations as defined above quantify the coherence in angular ordering of the UHECRs coming from the same source, and provide a separation of incoherently arriving UHECRs from different sources on a statistical basis.

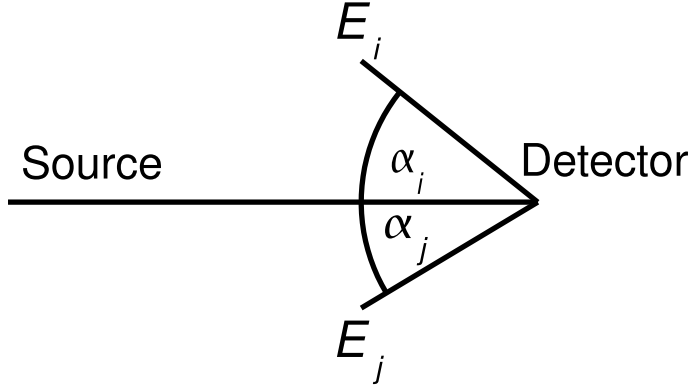


Figure 1: Schematic view of energy-energy-correlations

### 3. Analysis Method

#### 3.1. Signal Data Set

In order to evaluate the sensitivity of the energy-energy-correlation observable, we use instead of real data, a set of simulated UHECRs resulting from a source distribution. We will reference this in the following as signal data set.

Future Monte Carlo simulations of individual UHECRs aim to include specific candidate sources, a realistic distribution of galaxies, galaxy clusters and filaments, and a proper propagation through the corresponding media and magnetic fields. Here we use a simple representation of such a UHECR Monte Carlo generator which models the propagation process by a random walk. This can be considered to approximate at least the influence of extragalactic magnetic fields [9].

The random walk propagation is simulated by varying the angle  $\theta$  between the source direction and the arrival direction of the UHECR.  $\theta$  depends on the distance  $D$  which a proton propagates through magnetic fields of strength  $B$  in zones of the correlation length  $\lambda$ . The angle is chosen randomly according to a 2-dimensional Gaussian distribution with the width

$$\sigma_\theta \simeq 0.025 \text{ deg} \left( \frac{D}{\lambda} \right)^{1/2} \left( \frac{\lambda}{10 \text{ Mpc}} \right) \left( \frac{B}{10^{-11} \text{ G}} \right) \left( \frac{E}{10^{20} \text{ eV}} \right)^{-1}. \quad (2)$$

For the energy distribution of the UHECRs we follow the spectrum measured by the Pierre Auger Observatory [10],

$$J(E) \propto E^\gamma \quad (3)$$

with  $\gamma = -2.69$  for  $4 \text{ EeV} < E < 40 \text{ EeV}$ ,  $\gamma = -4.2$  for  $E > 40 \text{ EeV}$ .

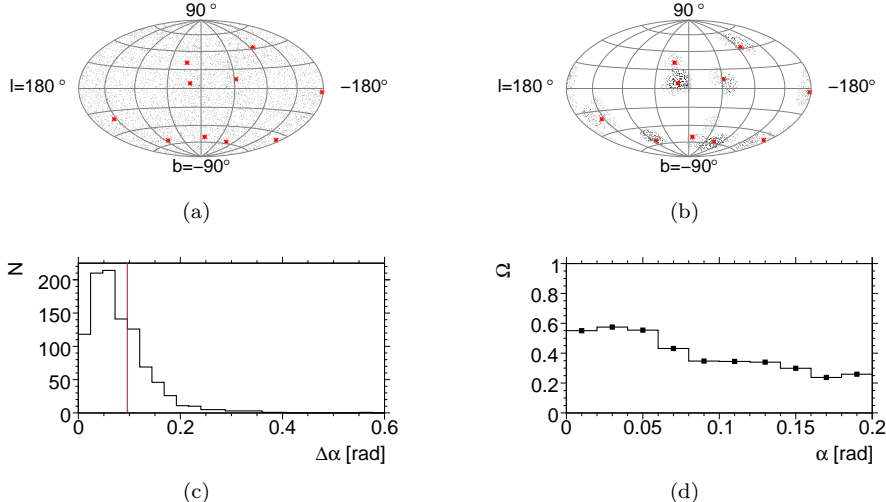


Figure 2: (a) Arrival directions of the signal data set (black point symbols) and the sources (red asterisk symbols), (b) UHECRs belonging to regions of interest (black point symbols) and the sources (red asterisk symbols), (c) Reconstruction quality of the source direction using the cone algorithm (red line: 68%-quantile), (d) Energy-energy-correlations of the signal data set

In the production of our signal data set we first generated 10 randomly distributed sources in the sky. We assumed that all sources have a similar distance to the earth such that equation 2 simplifies to

$$\sigma_\theta \simeq C_{Field} \left( \frac{E}{10^{18} \text{eV}} \right)^{-1}. \quad (4)$$

We produced the signal data set with  $C_{Field} = 10$  rad. A scenario compatible with this choice is e.g.,  $D = 50$  Mpc,  $\lambda = 1$  Mpc, and  $B = 3$  nG. We further assumed that all sources have identical luminosity and each of them emitted 1000 protons. The total signal data set amounts to 10000 UHECRs with energies above 5 EeV. In figure 2(a) we show the positions of the sources (asterisk symbols), and the resulting UHECR distribution (point symbols) as observed at the earth using the Hammer projection of the galactic coordinates. The UHECR distribution appears to be almost isotropic.

### 3.2. Regions of Interest

We define a ROI as a region that is close to a source of UHECRs. Since no UHECR source has been clearly identified so far, we will apply a simple iterative cone algorithm to find ROI's that have an increased probability to contain a source. The algorithm works as follows.

1. Select all UHECRs with energies above  $E_{min} = 60$  EeV as initial seeds,

2. For all seeds, define a corresponding ROI by assigning all UHECRs with angular distances less than  $\alpha_{max} = 0.2$  rad,
3. Calculate the center of mass of each ROI using the energies of the UHECRs as weights,
4. Use the center of mass of the ROI as a new seed, and iterate starting from item 2.

Note that in this algorithm every UHECR can be part of several ROIs. The algorithm is processed in total three times, and the last resulting ROIs are taken for further analysis.

In order to test the accuracy of reconstruction of a source direction with the ROI method, we produced 100 additional simulated data sets using the same magnetic field strength, and the same number of sources as above. We varied the random generator seeds to produce different source positions and UHECRs.

The performance of the ROI algorithm is shown in figures 2(b) and 2(c). In the signal data set all sources are covered by ROIs. Using the 100 additional data sets with the identical parameters, 95% of the sources are covered by ROIs. We obtain an angular resolution in terms of the 68%-quantile of 0.096 rad. Note that some reconstructed ROIs do not correspond to sources, and provide a background contribution to the following analysis.

### 3.3. Calculation of Energy-Energy-Correlations

In the next step we calculate the energy-energy-correlations of all pairs of UHECRs that belong to the same ROI. Each value of  $\Omega_{ij}$  (equation 1) is filled into a histogram for both angular distances  $\alpha_i$  and  $\alpha_j$ . Finally, in every angular bin of  $\alpha$  we calculate the average value  $\Omega$  and its uncertainty. In figure 2(d), we show the distribution of  $\Omega$  where we have included the  $\Omega_{ij}$  values of all ROIs simultaneously. The corresponding error bars are small compared to the size of the symbols. The result is the angular distribution of the energy-energy-correlations, which represents an estimator of coherence of the UHECR sky.

## 4. Evaluation of UHECR models

In this section we present a method of evaluating models of UHECR emission and propagation using an energy-energy-correlation measurement as presented above. As an example, we demonstrate the potential to exclude a model of isotropic arrival directions by comparison with the signal data distribution shown in figure 2(d). Furthermore, we evaluate variants of the above mentioned random walk model using different numbers of sources and magnetic field parameters. We demonstrate how phase space regions of possible parameter settings of this model can be excluded. Finally we quantify the precision of the reconstruction of these parameters.

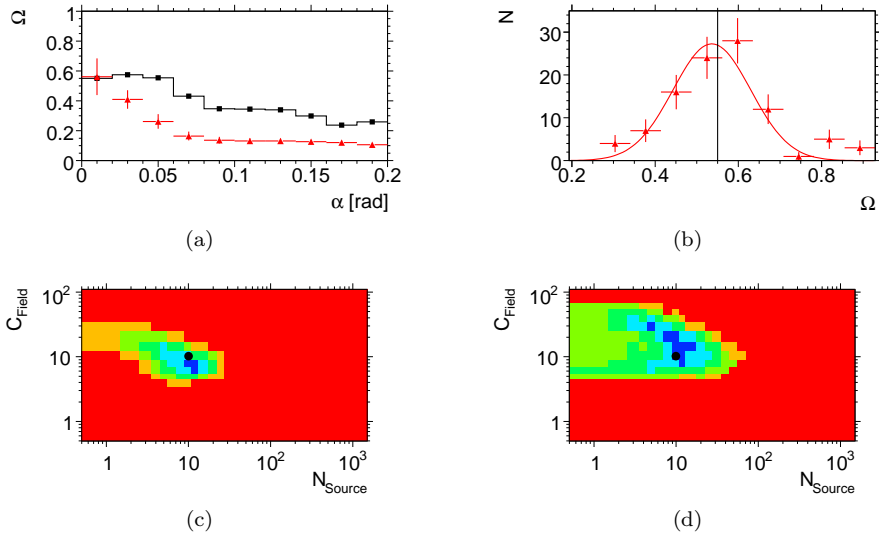


Figure 3: (a) Energy-energy-correlations of the signal data (black square symbols) compared with the result of isotropic arrival directions (red triangle symbols), (b)  $\Omega$ -distribution of the first bin of (a) (same color code), (c) Error contours for the reconstructed parameters resulting from the negative log-likelihood analysis (dark blue =  $1\sigma$ -contour, light blue =  $2\sigma$ -contour, dark green =  $3\sigma$ -contour, light green =  $4\sigma$ -contour, yellow =  $5\sigma$ -contour, red =  $> 5\sigma$ ), the black point symbol shows the parameters of the signal data set, (d) Error contours using 100 signal data sets (same color code as in (c))

#### 4.1. Isotropic UHECR Arrival Directions

We compare the energy-energy-correlations of the signal data with the hypothesis of isotropic arrival. We simulated 100 UHECR data sets with isotropic arrival directions. For each set we calculated the energy-energy-correlations as described in section 3. The average value of the resulting  $\Omega$ -distributions is shown in figure 3(a) as the triangle symbols. The error bars represent the spread of the average values of the individual distributions. The square symbols show the same signal data distribution as in figure 2(d).

In order to quantify the agreement of the isotropic arrival model with the signal data distribution we use the negative log-likelihood method. For the comparison of the distributions we take bin-by-bin correlations into account. We make use of the approximately Gaussian shape of the  $\Omega$  distributions within the angular  $\alpha$  bins (e.g. figure 3(b)), and define for the negative log-likelihood value

$$L = -2 \ln \left( \frac{\det(V^{-1})^{1/2}}{(2\pi)^{n/2}} \exp \left( -\frac{1}{2} (\mathbf{x} - \langle \mathbf{y} \rangle)^T \cdot V^{-1} \cdot (\mathbf{x} - \langle \mathbf{y} \rangle) \right) \right). \quad (5)$$

Here  $\mathbf{x}$  and  $\langle \mathbf{y} \rangle$  are  $n$ -dimensional vectors ( $n=10$ , the number of bins in figure 3(a)) containing the signal data values of each  $\alpha$  bin ( $\mathbf{x}$ ), and the mean of the isotropic distributions ( $\langle \mathbf{y} \rangle$ ).  $V$  is the covariance matrix of the histogram resulting from the isotropic model (figure 3(a)). The coefficients of  $V$  of the distribution  $\mathbf{y}$  are defined as follows,

$$V_{ij} = \langle y_i y_j \rangle - \langle y_i \rangle \langle y_j \rangle. \quad (6)$$

The resulting value of  $L = 133$  needs to be compared with an isotropic reference distribution in  $L$ . Using isotropic distributions instead of the signal data we obtain a narrow distribution centered at  $L_0 = -46$  with a root mean square of  $L_{RMS} = 5$ . The possibility of the signal data distribution to result from a fluctuation of isotropic distribution of UHECRs is therefore excluded with more than five standard deviations.

#### 4.2. Random Walk Model

In this section we confront a large number of variants of the random walk model with the signal data distribution (figure 2(d)). We vary the magnetic field as represented by the parameter  $C_{Field}$  of equation 4, and the number of sources  $N_{source}$  emitting UHECRs with the same luminosity. We keep the total number of UHECRs  $N_{UHECR} = 10000$  constant such that each source emits  $N_{UHECR}/N_{source}$  UHECRs.

In order to cover the relevant regions of the parameter space we chose an almost logarithmic binning with 25 different numbers of sources (between 1 and 10000), and 16 different values of  $C_{Field}$  (between 1 rad and 100 rad). For each of these values we simulated 100 random walk data sets, and determined the corresponding energy-energy-correlation distributions. The mean values  $\langle \mathbf{y} \rangle$  and the covariance matrix  $V$  are obtained for each pair of the model parameter values ( $N_{source}, C_{Field}$ ).

For these values we calculated the negative log-likelihood values  $L(N_{source}, C_{Field})$  according to equation 5 using for  $\mathbf{x}$  again the signal data of figure 2(d). In order to reduce fluctuations resulting from the finite number of random walk data sets in each  $(N_{source}, C_{Field})$  bin, we smoothed the bins of the  $L(N_{source}, C_{Field})$  distribution with a  $5 \times 5$ -kernel. The center weight of the kernel is  $K_{33} = 5$ . All neighbor weights of  $K_{33}$  have the weight  $K_{22} = K_{23} = K_{24} = K_{32} = K_{34} = K_{42} = K_{43} = K_{44} = 2$ , and all second neighbors have zero weight except  $K_{13} = K_{31} = K_{35} = K_{53} = 1$ . This means the value of every bin is replaced by a weighted mean of the neighboring bins, according to the weights of the kernel.

The result of this approximation is shown in figure 3(c). The red area indicates the region of the model parameters which are excluded at the level of more than five standard deviations.

The other contours in figure 3(c) represent levels of  $n$  standard deviations, with the inner dark blue region giving the result for  $n = 1$  standard deviation. The input parameters of the signal data set are shown by the point symbol. Its comparison with the standard deviation contours demonstrates that it is possible to reconstruct the number of sources, and the magnetic field strength of such a model at a reasonable level of precision.

Furthermore, we examined the potential of a systematic error resulting from the random seed of the signal data set. A simple example for such a systematic error would be two sources in the same line of sight, which would appear as one. We therefore repeated the analysis with 100 data sets with the same parameters as the signal data set, but with different random seeds. We averaged over all 100 negative log-likelihood distributions, and repeated the calculation of the error contours. In this case there is no need to apply a smoothing algorithm, since averaging over 100 distributions reduces the fluctuations. The contours are shown in figure 3(d) and have approximately the same size as in figure 3(c). This demonstrates that fluctuations within the signal data are reasonably small, and neither have a major influence on the precision of the exclusion region, nor on the quality of the reconstructed parameters.

## 5. Conclusions

In this paper we introduced an energy-energy-correlation observable  $\Omega$  designed to obtain information on sources and propagation of UHECRs. We have also presented a likelihood method to evaluate models of UHECR emission and propagation using  $\Omega$  measurements. To check the sensitivity of the analysis procedure, we compared simple models with a simulated  $\Omega$  measurement. We demonstrated that the phase space of model parameters, the number of sources and a parameter reflecting the average magnetic field strength, could be constrained with reasonable precision.

## 6. Acknowledgments

We wish to thank Johannes Erdmann for fruitful discussions, and a cross-check of the random generators. We are grateful to the Pierre Auger magnetic fields group and to the local group from Aachen for valuable discussions. We also thank Christopher Wiebusch for valuable comments on this publication. This work is supported by the Ministerium für Wissenschaft und Forschung, Nordrhein-Westfalen, and the Bundesministerium für Bildung und Forschung (BMBF).

## References

- [1] The Pierre Auger Collaboration 2007, *Science*, 318 (5852), 938
- [2] The Pierre Auger Collaboration, 2008, *Astropart. Phys.*, 29, 188-204
- [3] Beck, R. 2008, *Proceedings of the 4th International Meeting on High Energy Gamma-Ray Astronomy*, Heidelberg, Germany, AIP Conf. Proc., Volume 1085, 83-96
- [4] Han, J.L. 2009, arXiv:0901.1165v1, to be published in *Proceedings of the IAU Symposium*, Tenerife, Spain, No. 259
- [5] Sigl, G., et al. 2004, *Nuclear Physics B - Proceedings Supplements*, 136, 224-233
- [6] Dolag, K., et al. 2005, *JCAP*, 01, 009
- [7] Ryu, D., et al. 2008, *Science*, 320 (5878), 909
- [8] H1 Collaboration 1996, *Z. Phys. C*, Vol. 70, No. 1, 17-30
- [9] Waxman, E., Miralda-Escude, J. 1996, *Astrophys. J. Lett.*, 472, L89
- [10] The Pierre Auger Collaboration, 2008, *Phys. Rev. Lett.*, 101, 061101